# Sub-arcsecond imaging at 267 GHz of a young binary system: Detection of a $< 70$ AU radius dust disk around T Tau N

Michiel R. Hogerheijde[1], Huib Jan van Langevelde[2], Lee G. Mundy[3], Geoffrey A. Blake[4], and Ewine F. van Dishoeck[1]

## ABSTRACT

The young binary system T Tau was observed with the Owens Valley Millimeter Array in 267 GHz continuum and $HCO^+$ $J$=3–2 emission at 0.″8 resolution, with the JCMT–CSO single-baseline interferometer in 357 GHz continuum, and with the W. M. Keck telescope at $\lambda$=4 $\mu$m. The 267 GHz emission is unresolved with a flux of $397 \pm 35$ mJy, located close to the position of the optical star T Tau N. An upper limit of 100 mJy is obtained toward the infrared companion T Tau S. The 357 GHz continuum emission is unresolved, with a flux of $1.35 \pm 0.68$ Jy. $HCO^+$ $J$=3–2 was detected from a 2″ diameter core surrounding T Tau N and S. Both stars are detected at 4 $\mu$m, but there is no evidence of the radio source T Tau R.

We propose a model in which T Tau S is intrinsically similar to T Tau N, but is obscured by the outer parts of T Tau N's disk. A fit to the spectral energy distribution (SED) between 21 cm and 1.22 $\mu$m is constructed on this basis. Adopting a $r^{-1}$ surface density distribution and an exponentially truncated edge, disk masses of $0.04 \pm 0.01$ $M_\odot$ and $6 \times 10^{-5} - 3 \times 10^{-3}$ $M_\odot$ are inferred for T Tau N and T Tau S, respectively. A 0.005–0.03 $M_\odot$ circumbinary envelope is also required to fit the millimeter to mid-infrared SED.

*Subject headings:* ISM: molecules — stars: formation — stars: low mass, brown dwarfs — stars: pre–main sequence — binaries: close

## 1. Introduction

Many low-mass stars form in multiple systems (cf. Ghez et al. 1993), either through capture, fragmentation of the collapsing core, or condensation from the primary's disk (e.g., Bodenheimer, Ruzmaikina & Mathieu 1993). The presence of a close companion must influence the evolution of

[1]Sterrewacht Leiden, P.O. Box 9513, 2300 RA, Leiden, The Netherlands

[2]Joint Institute for VLBI in Europe, P.O. Box 2, 7990 AA, Dwingeloo, The Netherlands

[3]Department of Astronomy, University of Maryland, College Park, MD 20742

[4]Division of Geological and Planetary Sciences, California Institute of Technology, MS 150–21, Pasadena, CA 91125

the star and the possible development of an accretion disk (e.g., Jensen et al. 1996). Observations of the distribution of the bulk of the gas and dust in young and forming multiple systems are needed to better understand their evolution, which may be very different from that of a single star. This Letter presents high resolution continuum and spectral line observations of one such close multiple system: T Tauri.

A prototypical low-mass young stellar object (YSO), T Tau is a 0.″7 separation binary (projected distance of 100 AU at 140 pc), consisting of an optically visible star, T Tau N, and an infrared companion, T Tau S (Dyck, Simon & Zuckerman 1982). Ray et al. (1997) report the presence at $\lambda = 6$ cm of a third source, possibly a star, T Tau R. The system is surrounded by 0.03 to 0.3 $M_\odot$ of gas and dust distributed on 3000 to $10^4$ AU scales (e.g., Schuster, Harris & Russell 1997; Hogerheijde et al. 1997). Both stars appear to drive outflows, at least one of which is directed close to the line of sight (Edwards & Snell 1982, Beckwith et al. 1978; van Langevelde et al. 1994; Herbst et al. 1997). Stellar light curves indicate that the rotation axis of T Tau N is inclined by only $\sim 19°$ (Herbst et al. 1997). From the strength and variability of its free-free radio emission, T Tau S appears to be a more active outflow source than T Tau N (Skinner & Brown 1994; Ray et al. 1997).

The infrared nature and activity of T Tau S have been explained in a number of ways: through obscuration by a remnant protostellar envelope surrounding T Tau S (Dyck et al. 1982) or around the binary system (Calvet et al. 1994), or through obscuration caused by periodic perturbation of circumstellar material in the binary orbit (Koresko, Herbst & Leinert 1997). Until recently, the T Tau binary has only been resolved at centimeter and near-infrared wavelengths. All information on the gas and dust in the system has been derived from (sub-)millimeter and far-infrared measurements, which did not separate the pair. In this Letter we present sub-arcsecond resolution 267 and 357 GHz continuum observations showing that the compact dust emission from the system is confined to the surroundings of T Tau N (see also van Langevelde et al. 1997). In addition, 0.″4 resolution imaging confirms that T Tau S is brighter than T Tau N at $\lambda$=4 $\mu$m. The spatially resolved (sub-)millimeter fluxes, and literature values for centimeter and infrared observations, allow a fit to the spectral energy distributions (SEDs) of the individual sources, constraining the mass and size of the disk around T Tau N and the circumstellar material around T Tau S.

## 2. Observations

Continuum emission at 267 GHz and $HCO^+$ $J$=3–2 line emission were imaged with the Millimeter Array at the Owens Valley Radio Observatory (OVRO) on 1994, December 1. Baselines between 20 and 200 k$\lambda$ were sampled, resulting in a 0.″77 × 0.″96 synthesized beam for a robust weighting of +1. The continuum data were integrated over a 1 GHz band width, yielding a 1$\sigma$ RMS noise level of 30 mJy bm$^{-1}$. The $HCO^+$ 3–2 data were recorded in a 64 channel correlator with a resolution of 0.5 MHz or 0.56 km s$^{-1}$; the 1$\sigma$ RMS noise in a channel is 1.3 Jy bm$^{-1}$, or 19 K km s$^{-1}$ for natural weighting. The antenna-based complex gains of the OVRO instrument

were derived with the MMA package, using PKS 0528+134 as the phase calibrator and 3C 454.3 as the flux calibrator, for which a flux of 6.50 Jy was derived from observations of planets. The data were mapped and analyzed with the MIRIAD software package. Like the radio positions of T Tau N and S, the coordinates of the 267 GHz emission are tied to the radio reference frame; the estimated uncertainty in the absolute positions of 0.″2 is dominated by the accuracy of the array baselines.

The 357 GHz continuum emission was observed together with $HCO^+$ 4–3 line emission using the single-baseline interferometer (SBI) of the James Clerk Maxwell Telescope (JCMT) and the Caltech Submillimeter Observatory (CSO), on 1994, October 28. Projected baselines ranged between 140 and 195 k$\lambda$, resulting in an effective resolution of $\sim$ 0.″7. The data were recorded in a 500 MHz wide band with 400 channels, and vector-averaged over 100 second intervals. The gain of the instrument was $\sim$ 135 Jy $K^{-1}$, derived from PKS 0528+134. Since the phase variations on the JCMT–CSO baseline cannot be tracked, only the 100 s vector-averaged visibility amplitudes are used (cf. Lay et al. 1994).

Imaging at $\lambda$=4 $\mu$m was acquired with the W. M. Keck Telescope on 1997, February 7, using the Near Infrared Camera and Br$\alpha$–continuum filter (3.97–4.02 $\mu$m). The detector array has 0.″15 pixels. The final image contains 2000 integrations of 45 milliseconds each. Atmospheric conditions were good, with a seeing of 0.″3–0.″4. The image was processed with the IRAF package.

## 3. Results

The 267 GHz continuum emission, shown in Fig. 1a, is unresolved with a peak flux of $369 \pm 30$ mJy $bm^{-1}$. A point-source fit to the visibilities yields a flux of $397 \pm 35$ mJy, and a position within 1$\sigma$ (0.″2) of both T Tau N and T Tau R (Table 1). The 3$\sigma$ upper limit on the flux toward T Tau S is 100 mJy. Although T Tau R, at 0.″13, is slightly closer to the continuum peak than T Tau N (0.″20), we attribute the 267 GHz emission to T Tau N, due to the uncertain nature of T Tau R. Based on the compactness of the source and the emission at infrared and sub-millimeter wavelengths (Herbst et al. 1997; Beckwith et al. 1990), we interpret the 267 GHz emission as arising from a disk of radius $< 0.''45 \approx 70$ AU around the optical star.

The $\lambda$=4 $\mu$m Keck image of the T Tau system is shown in Fig. 1b in grey scale, with contours of the 267 GHz emission superposed. The binary is clearly resolved and is consistent with two individual point sources. The 4 $\mu$m flux from T Tau S is 1.5 times that from T Tau N. No absolute positional information is available for the Keck data, so the image has been aligned with the radio positions of T Tau. The binary separation at 4 $\mu$m is 0.″70, consistent with measurements at centimeter wavelengths. No evidence is found for emission from T Tau R.

The 357 GHz continuum SBI data are consistent with emission from a single point source and yield a vector-averaged flux of $1350 \pm 675$ mJy, where the uncertainty is dominated by the flux calibration. The observed emission at 267 and 357 GHz accounts for 60%–80% of the single-dish

fluxes at these wavelengths on 19″ and 13″ scales, respectively (Moriarty-Schieven et al. 1994). Including the 2.7 mm point-source flux from Hogerheijde et al. (1997), a spectral index of $2.6 \pm 0.2$ is found for the compact emission.

Emission in the $HCO^+$ 3–2 line is detected only on baselines $< 70$ k$\lambda$, and over 3–11 km s$^{-1}$. The naturally weighted image (Fig. 1c) shows a 2″ core, centered between T Tau N and S, with a peak flux of $6.1 \pm 0.4$ Jy bm$^{-1}$ or 745 K km s$^{-1}$. This is 25% of the 19″ single-dish line flux, comparable to the 10% recovered at $HCO^+$ 1–0 by OVRO (Hogerheijde et al. 1998). No emission from $HCO^+$ 4–3 was detected in the SBI data with a statistical upper limit of $\sim 0.35$ Jy, or $\sim 7$ K, for a 1″ source size, consistent with the non-detection of $HCO^+$ 3–2 emission on baselines $> 70$ k$\lambda$.

## 4. Understanding the nature of T Tau S and T Tau N

Our observations of 267 GHz continuum emission show that most of the material on 100 AU scales is associated with T Tau N, most likely in a disk. Although the near-infrared SED of T Tau S also indicates the presence of a disk, the 267 GHz upper limit strictly constrains the mass. Bate & Bonnell (1997) found that material infalling toward a binary system preferably forms a disk around the more massive primary, which our observations show to be T Tau N. How does the difference in disk mass for T Tau N and S impact our understanding of the T Tau system, especially the obscured, infrared nature of T Tau S?

Of the many scenarios which have been proposed to explain the infrared nature of T Tau S (see §1), that of dynamical interaction is particularly interesting because it links the obscuration of infrared companions in binary systems with their observed variability (Koresko et al. 1997). Based on our new data for T Tau, we propose a variation on this model, wherein T Tau S is obscured directly by the disk around T Tau N. This requires the disk to extend to $\gtrsim 100$ AU, at a modest inclination with respect to the binary orbital plane. For the assumed dust properties (Ossenkopf & Henning 1994; their model 'thin 6'), a surface density of 0.12 g cm$^{-2}$ is required to obscure an assumed stellar photosphere for T Tau S of $\sim 5000$ K.

To further investigate this model and derive mass estimates for the disks around T Tau N and S, and for the circumbinary envelope, a fit to the SED between 21 cm and 1.22 $\mu$m is constructed (Fig. 2). The model for T Tau N is based on a stellar photosphere of 5250 K (K0 star), and a temperature distribution in the disk characterized by a radial power law with index $-q$ with an intrinsic luminosity $L_{\rm d}$ (Adams, Lada & Shu 1987; eq. [A22]). From the optically thick 1.22 to 20 $\mu$m range, estimates are obtained of the stellar radius, $R_* = 3.4\ R_\odot$, the inner radius of the disk, $R_{\rm in} = 5.1\ R_\odot$, the disk luminosity, $L_{\rm d} = 3.0\ L_\odot$, and the index, $q = 0.51$ (cf. Herbst et al. 1997).

At longer wavelengths, where the disk is largely optically thin, the surface density is important. The density distribution depends on angular momentum transport processes like viscosity and disk wind (cf. Adams & Lin 1993). The gravitational interaction with the binary companion is expected to truncate the disk at some radius (cf. Lin & Papaloizou 1993). The

surface density is approximated here by a radial power law $\Sigma \propto r^{-1}$, which is truncated at radii $r > R_{\rm trunc}$ by an exponential taper, $\exp[-(r - R_{\rm trunc})/r_e]$. It is found that this exponential fall-off is required to permit the low surface density of 0.12 g cm$^{-2}$ needed for the obscuration of T Tau S while and still fitting the flux of T Tau N. The exact functional form of the truncation or the adopted outer radius is not important for the derived masses for $R_{\rm trunc} \gtrsim 50$ AU. Assuming $R_{\rm trunc} = 70$ AU, the only free model parameter left is the $\frac{1}{e}$ radius $r_e$. The 267 GHz flux constrains $r_e$ to 7–8 AU, with a corresponding disk mass of $0.04 \pm 0.01\ M_\odot$.

The SED of T Tau S is fitted with the same model and parameters, plus obscuration by the disk of T Tau N. The only differences are the disk mass, along with the luminosity of 15 $L_\odot$ and index of q=0.54 required to fit the higher infrared fluxes. An interstellar extinction of $A_V$=1.44 mag is applied to the whole system (Cohen & Kuhi 1979), and free-free spectral indices of 0.6 and 0.2 are used for T Tau N and S, respectively. The assumed stellar temperature is unimportant since the disk luminosity dominates the SED at $\lambda > 2\ \mu$m. The disk mass is constrained by the 20 $\mu$m flux and the 267 GHz upper limit to lie between $6 \times 10^{-5} - 3 \times 10^{-3}\ M_\odot$.

To fit the unresolved (sub-)millimeter and infrared observations, a circumbinary envelope of 0.005–0.03 $M_\odot$ is also required, depending on the disk mass of T Tau S. This envelope is modeled with a power law for the density with slope $p = -1.5$, and for the temperature with slope $q = -0.4$. At the inner radius of 100 AU, a temperature of 63 K provides a good fit to the peak of the SED. An outer radius of 3000 AU is used, corresponding to the typical beam size of the (sub-)millimeter observations. The presence of this power-law envelope is consistent with the non-detection of extended 267 GHz continuum emission on 16–200 k$\lambda$ baselines at the obtained noise level. The $HCO^+$ 3–2 emission on 16–70 k$\lambda$ baselines can be explained by the sensitivity of this line to density, which results in a more peaked brightness distribution, although additional emission from, e.g., material in the walls of the outflow cavity (cf. Hogerheijde et al. 1998) is required to fit its absolute flux.

The non-detection of $HCO^+$ 3–2 on baselines > 70 k$\lambda$ with an upper limit of $\sim 1.4$ Jy bm$^{-1}$, or $\sim 171$ K km s$^{-1}$, sets a rough upper limit to the $HCO^+$ abundance in the disk. Assuming an excitation temperature of 60 K and neglecting any optical depth effects, an upper limit to the abundance of $1 \times 10^{-8}$ is found.

The limit placed on the amount of circumstellar material around T Tau S by our 267 GHz measurements places constraints on the nature of the obscuration. While a small edge-on disk around T Tau S could provide the observed extinction, the disk around T Tau N is a more likely candidate. In either case, it is implied that the binary orbit and the respective disks are not coplanar. A circumstellar envelope around T Tau S alone is unlikely as obscuring agent, since it implies that either the current projected binary separation is a chance close projection, or that the envelope is < 50 AU and hence dynamically short-lived. An envelope around both T Tau N and S requires a special geometry which allows T Tau N to suffer little extinction while heavily obscuring T Tau S.

To test the hypothesis that T Tau N's disk is obscuring T Tau S, sub-arcsecond resolution observations at sub-millimeter wavelengths and at 10–20 $\mu$m are needed to place firmer limits on the distribution of the circumstellar material around T Tau S. For example, monitoring of the near-infrared variability and the shape of the 10 $\mu$m silicate absorption could distinguish intrinsic variations in T Tau S from inhomogeneities in the obscuring disk or changes in the star–disk geometry. Observation of the 20–200 $\mu$m spectrum planned for the *Infrared Space Observatory* will help to further constrain the SED model, since the emission from the disks and the envelope peak at these wavelengths. Some of the other infrared companions to T Tauri stars might be explained by disk obscuration as well (e.g., Haro 6–10 at $1\farcs2$ separation, Leinert & Haas 1989; XZ Tau at $0\farcs3$, Haas et al. 1990; UY Aur at $0\farcs9$, Herbst et al. 1995). Millimeter observations at sub-arcsecond resolution are needed to determine the material distributions in these systems.

The authors wish to thank O. Lay for a critical reading of the manuscript, and him and J. Carlstrom for assistance in the observation and reduction of the SBI data. The telescope staffs are thanked for support during the observations. E. v. D. acknowledges support by NWO/NFRA, G. A. B. by NASA (NAGW–2297, NAGW–1955), L. G. M. by NASA (NAG 5–4429), H. J. v. L. by the European Union (CHGECT920011). The OVRO Millimeter Array and the CSO are operated by the Caltech under funding from the NSF (AST96–13717, AST93–13929). The JCMT is operated by JAC on behalf of PPARC UK, NWO Netherlands, and NRC Canada. The W. M. Keck Observatory is operated as a scientific partnership between Caltech, Univ. of California, and NASA. It was made possible by the generous financial support of the W. M. Keck Foundation.

## REFERENCES


Adams, F. C., Lada, C. J., & Shu, F. H. 1987, ApJ, 312, 788

Adams, F. C., & Lin, D. N. C. 1993, in Protostars & Planets III, eds. E. H. Levy, J. I. Lunine (Tucson: Univ. Arizona), 721

Bate, M.R., & Bonnell, I.A. 1997, MNRAS, 285, 33

Beckwith, S., Gatley, I., Matthews, K., & Neugebauer, G. 1978, ApJ, 223, L41

Beckwith, S. V. W., Sargent, A. I., Chini, R. S., & Güsten, R. 1990, AJ, 99, 924

Beckwith, S. V. W., & Sargent, A. I. 1991, ApJ, 381, 250

Bodenheimer, P., Ruzmaikina, T., & Mathieu, R.D. 1993, in Protostars and Planets III, eds. E. H. Levy, J. I. Lunine (Tucson: Univ. Arizona), 367

Calvet, N., Hartmann, L., Kenyon, S.J., & Whitney, B.A. 1994, ApJ, 434, 330

Cohen, M., & Kuhi, L. V. 1979, ApJS, 41, 743

Dyck, H. M., Simon, T., & Zuckerman, B. 1982, ApJ, 255, L103

Edwards, S., & Snell, R. L. 1982, ApJ, 261, 151

Ghez, A. M., Neugebauer, G., & Matthews, K. 1993, AJ, 106, 2005

Haas, M., Leinert, Ch., Zinnecker, H. 1990, A&A, 230, L1

Herbst, T. M., Koresko, C. D., Leinert, Ch. 1995, ApJ, 444, L93

Herbst, T. M., Robberto, M., & Beckwith, S.V.W. 1997, AJ, 114, 744

Hogerheijde, M. R., van Dishoeck, E. F., Blake, G. A., & van Langevelde, H. J. 1997, ApJ, 489, in press

Hogerheijde, M. R., et al. 1998, in preparation

Jensen, E. L. N., Mathieu, R. D., & Fuller, G. A. 1996, ApJ, 458, 312

Koresko, C. D., Herbst, T. M., & Leinert, Ch. 1997, ApJ, 480, 741

Lay, O. P., Carlstrom, J. E., Hills, R. E., & Phillips, T. G. 1994, ApJ, 434, L75

Leinert, Ch., & Haas, M. 1989, ApJ, 342, L39

Lin, D. N. C., & Papaloizou, J. C. B. 1993, in Protostars & Planets III, eds. E. H. Levy, J. I. Lunine (Tucson: Univ. Arizona), 749

Moriarty-Schieven, G. H., Wannier, P. G., Keene, J., & Tamura, M. 1994, ApJ, 436, 800

Ossenkopf, V., & Henning, Th. 1994, A&A, 291, 943

Ray, T. P., Muxlow, T. W. B., Axon, D. J., Brown, A., Corcoran, D., Dyson, J., & Mundt, R. 1997, Nature, 385, 415

Schuster, K.-F., Harris, A. I., & Russell, A. P. G. 1997, A&A, 321, 568

Skinner, S. L., & Brown, A. 1994, AJ, 107, 1461

van Langevelde, H. J., van Dishoeck, E. F., van der Werf, P. P., & Blake, G. A. 1994, A&A, 287, L25

van Langevelde, H. J., van Dishoeck, E. F., & Blake, G. A. 1997, in CO: Twenty-five Years of Millimeter-wave Spectroscopy, Proc. IAU Symp. 170, eds. W. B. Latter et al. (Dordrecht: Kluwer), 469

Weintraub, D. A., Masson, C. R., Zuckerman, B. 1987, ApJ, 320, 336

Weintraub, D. A., Sandell, G., & Duncan, W. D. 1989, ApJ, 340, L69

This preprint was prepared with the AAS LaTeX macros v4.0.

Fig. 1.— (*a*) Cleaned image of 267 GHz continuum emission of T Tau using robust weighting of +1. Contours are drawn at $3\sigma$ intervals of 90 mJy bm$^{-1}$. T Tau N and S are indicated by crosses, T Tau R by an asterisk. (*b*) Same 267 GHz contours overlaid on the 4 $\mu$m image (grey scale), which has been aligned with the radio positions of T Tau N and S. (*c*) Velocity integrated $HCO^+$ 3–2 emission on baselines $< 120$ k$\lambda$. Contours are drawn at $3\sigma$ intervals of 9.2 Jy bm$^{-1}$ km s$^{-1}$ (134 K km s$^{-1}$).

Fig. 2.— Spectral energy distribution of T Tau N (*top panel*) and S (*lower panel*), and model curves for T Tau S $M_{\rm d} = 5 \times 10^{-4}$ $M_\odot$, and envelope $M = 0.02$ $M_\odot$. The data points include our 267 GHz and 357 GHz measurements and literature data (Beckwith et al. 1990; Beckwith & Sargent 1991; Herbst et al. 1997; Hogerheijde et al. 1997; Ray et al. 1997; Skinner & Brown 1994; Weintraub, Sandell & Duncan 1989; Weintraub, Masson, & Zuckerman 1987). The model is discussed in the text.

Fig. 1

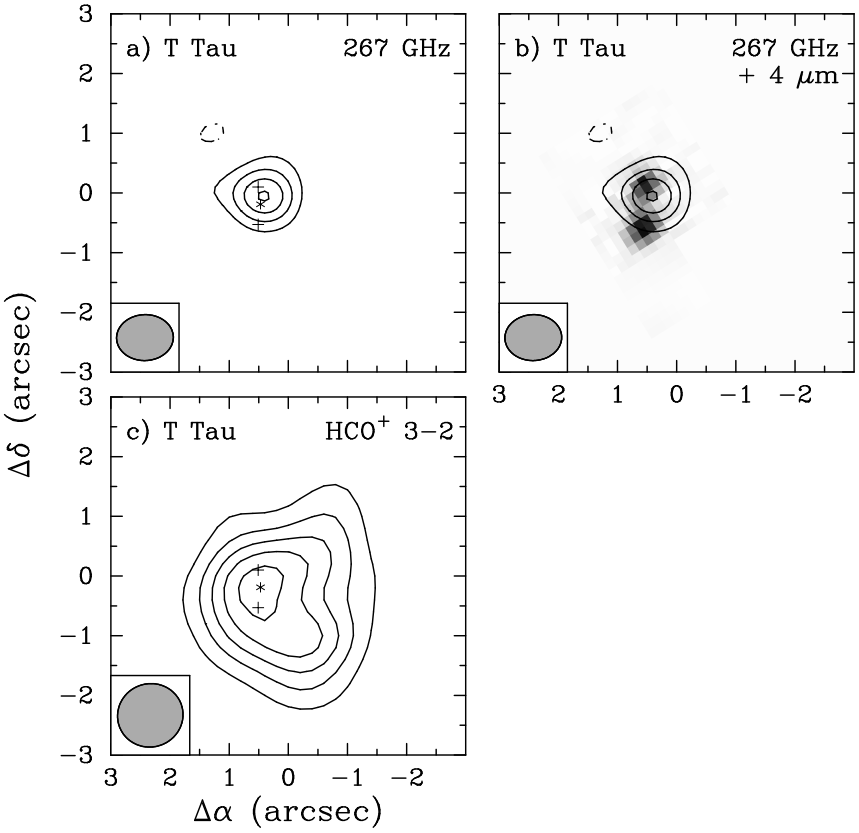
a) T Tau
267 GHz
b) T Tau
267 GHz
+ 4 μm
c) T Tau
HCO+ 3−2
Δδ (arcsec)
Δα (arcsec)
3
2
1
0
−1
−2
−3

Table 1. Source positions and 267 GHz fluxes[a]

| Source | $\alpha(1950.0)$ (hh mm ss) | $\delta(1950.0)$ (° ′ ″) | $F_\nu$ (Jy) |
|---|---|---|---|
| T Tau N | 04 19 04.24 | +19 25 04.92 | $0.397 \pm 0.035$ |
| T Tau S | ··· | ··· | $< 0.10$ |
| $HCO^+$ 3–2 | 04.19 04.23 | +19 25 04.46 | $29.5 \pm 2.8$ |
| Radio positions | | | |
| T Tau N[b] | 04 19 04.245 | +19 25 05.20 | |
| T Tau S[b] | 04.19 04.250 | +19 25 04.58 | |
| T Tau R[c] | 04.19 04.243 | +19 25 04.88 | |

[a]Absolute positional accuracy at 267 GHz $\sim 0\farcs2$.

[b]3.6 cm coordinates from Skinner & Brown 1994.

[c]6.0 cm coordinates from Ray et al. 1997.

Fig. 2

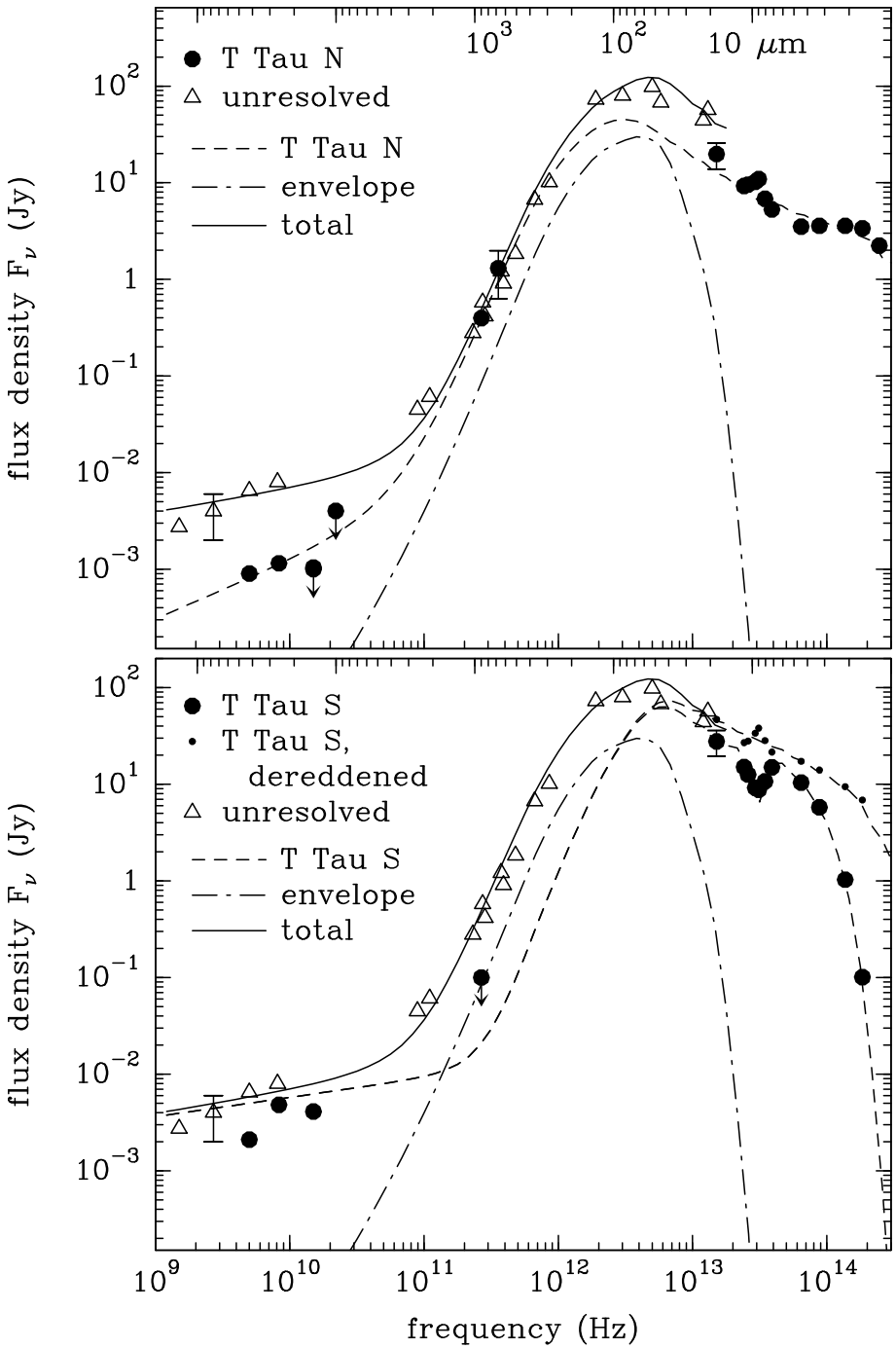
T Tau N
unresolved
T Tau N
envelope
total
10 μm
flux density $F_\nu$ (Jy)
T Tau S
T Tau S, dereddened
unresolved
T Tau S
envelope
total
flux density $F_\nu$ (Jy)
frequency (Hz)